ACS Macro Letters

Letter

pubs.acs.org/macroletters

Long-Range Ordered Crystallization Structure in the Micromolded Diblock Copolymer Thin Film

Peng Zhang,[†] Haiying Huang,[†] Tianbai He,*[,†] and Zhijun Hu*[,‡]

[†]State Key Laboratory of Polymer Physics and Chemistry, Changchun Institute of Applied Chemistry, Graduate School of the Chinese Academy of Sciences, Chinese Academy of Sciences, Changchun 130022, People's Republic of China

[‡]Center for Soft Condensed Matter Physics and Interdisciplinary Research, Soochow University, Suzhou 215006, People's Republic of China

Supporting Information

ABSTRACT: Confined crystallization of the micromolded poly(butadiene)-*block*-poly(ε-caprolactone) (PB-*b*-PCL) diblock copolymer thin film was studied in this work. The long-range regular ordering of the PCL crystal with crystallographic *b*-axis parallel to the long-axis of the channel was detected, as indicated by the electron diffraction and grazing-incidence X-ray diffraction experimental results. This preferential crystallographic orientation is mainly because that PCL block crystallization was readily influenced by the geometric effect, then, the fast-growth direction (crystallographic *b*-axis) was forced to extend along the long-axis of the channel to grow long. Moreover, the substrate induced ordering of the block copolymer restricted the "in-plane" molecular diffusion in the residual layer, and cross-channel crystallization was precluded. Hence, micromolding seems to be a promising method for tailoring the nanoscale crystallization of block copolymer in thin films.

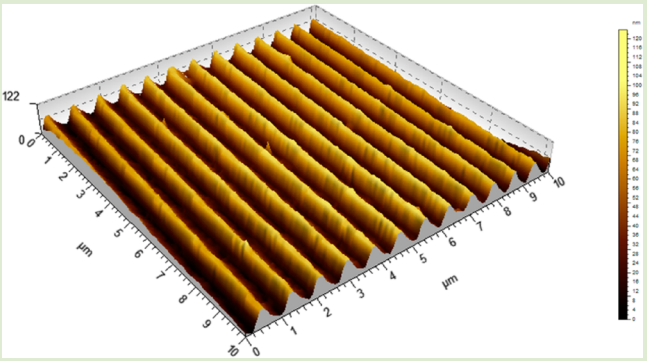

Semicrystalline polymers typically organize into multiscale polycrystalline spherulites that are comprised of splaying and branching lamellae interleaved with amorphous layers. The typical thickness of lamellar crystals lies in the nanometer scale, while the lateral dimensions are in the micrometer scale.[1] Thus, the crystalline structures of semicrystalline polymers span a wide range of length scales. It can be obviously predicted that mesoscale confinement can strongly perturb the crystalline process at different length scales, affecting the crystal nucleation, growth of individual lamellae, as well as the final morphologies. This has been convinced in the crystallization of different confined-geometries such as the nanodomains of block copolymers,[2−10] in droplets,[11,12] and mold for nanoimprinting[13−18] or porous templates.[19−22] In the case of microphase-separated block copolymers, only nanoscopic confinement (<100 nm) from chemical links between different blocks is provided. Micromolding, however, offers a versatile tool to study the crystallization of polymers under physical confinement, because the confinement can span a wide range of sizes from nanometer to micrometer, depending on the designed mold.

In this letter, we report on the crystallization of microphase-separated block copolymers under the confinement of a few hundred nanometers. Cylindrical poly(butadiene)-*block*-poly(ε-caprolactone) (PB-*b*-PCL) with PCL being the minority component was selected because of the following reasons. First, the PCL is recognized as an alternative model of the polyethylene, the well studied "model" semicrystalline polymer.[3−5,8,12,19,20,23] Second, despite the hard confined crystallization of PCL in the poly(4-vinylpyridine)-*block*-poly(ε-caprolactone)[7] and poly(styrene)-*block*-poly(ε-caprolactone) (PS-*b*-PCL),[24] PB-*b*-PCL is a typical soft-confined system for which crystallization occurs when the amorphous block is in the rubbery state and the final morphology is dominated by the crystallization.[25] Finally, PCL crystal form does not change with the confined environment, which offers a convenient system for the practical experimental reasons.[6,24,26,27]

A PB-*b*-PCL with weight and number average molecular weights of 22990 and 20900 g/mol was purchased from Polymer Source, Inc., and used as received. The volume fraction of PCL (f_{PCL}) is 32.6%, which corresponds to a cylinder microphase structure.[28] Thin films were obtained by spin-casting toluene solution (20 mg/mL) onto clean silicon and carbon-coated mica wafers, following the removal of solvent in vacuum for 24 h.

The mold used in this study was cross-linked poly(dimethyl siloxane) (PDMS; Sylgard 184, Dow Corning Co.). Figure 1a shows the morphology of the patterned PDMS mold, characterized with atomic force microscope (AFM; SPA-300HV, Seiko, Japan). It is consisted of parallel line-grating

Received: June 2, 2012
Accepted: July 17, 2012
Published: July 20, 2012

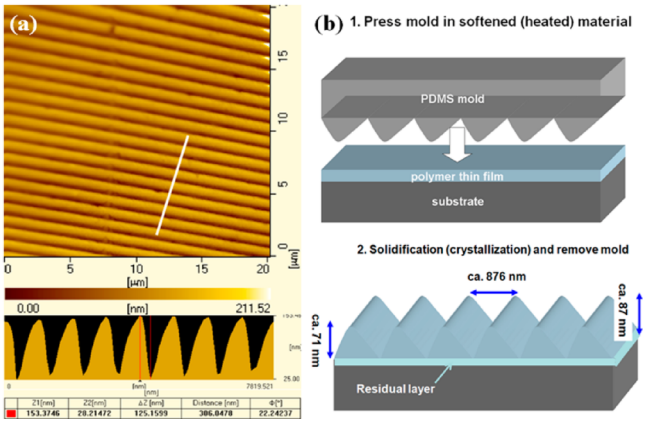

Figure 1. (a) AFM height image of the PDMS mold, the lower part offers the height fluctuations corresponding to the white line section. (b) Schematic drawing of the micromolding process.

patterns with a periodicity of about 870 nm. The cross-section is a sawtooth pattern with the maximum height of 125 nm. The micromolding was performed in a homemade micromolder, equipped with water and liquid-nitrogen cycle refrigeration components. Figure 1b shows the schematic drawing of molding process. The sample was imprinted at 150 °C and kept for 30 min before being cooled to room temperature. The sample was kept at room temperature (ca. 25 °C) for 24 h to crystallize, being solidified, after which the pressure (ca. 0.7 MPa) was released and the mold was removed. In addition, on the basis of the cross-sectional analysis results, height and periodicity values of the replicated pattern were around 71 and 876 nm, respectively. The maximum height of the imprinted line was about 87 nm, measured with AFM by scratching method. Comparing height values, it is easy to find that there was a residual layer with thickness about 16 nm lying around the substrate.

Figure 2 shows the surface morphology of the PB-*b*-PCL thin films before and after micromolding. In Figure 2a, the

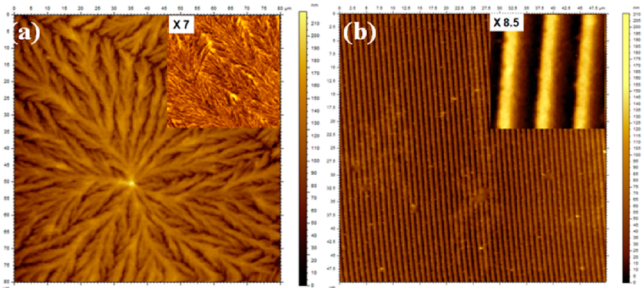

Figure 2. AFM height images of the (a) unmolded (the inset is the 7× magnified phase image) and (b) molded (the inset is the 8.5× magnified height image) PB-*b*-PCL thin films. The scanning areas in panels a and b are 80 × 80 and 50 × 50 μm, respectively.

unmolded PB-*b*-PCL thin film shows spherulite morphology. The formation of spherulite was because crystallization destroyed the microphase structure and dominated the final morphology.[28] Moreover, as shown in the inset of Figure 2a, the spherulite is composed of secondary lamellae unit. However, it is hard to ascertain the lamellae take flat-on (with the crystallographic *c*-axis, chain stem, normal to the substrate) or edge-on (with the crystallographic *c*-axis parallel to the substrate) orientation simply from the surface morphology observation. Figure 2b displays regular line-grating pattern for the micromolded PB-*b*-PCL thin film. The formation of regular patterns implied that the crystallization was dominantly disturbed by the molded lines. Especially, as shown in the inset of Figure 2b, there is no crystallization-induced corrugation observed in the sample surface, indicating that crystallization was confined in the channels.

To study the crystalline morphology within the film, further characterization was performed with transmission electron microscope (TEM; JEOL JEM 1011) because AFM only offered the free surface profile. Figure 3 reveals that the

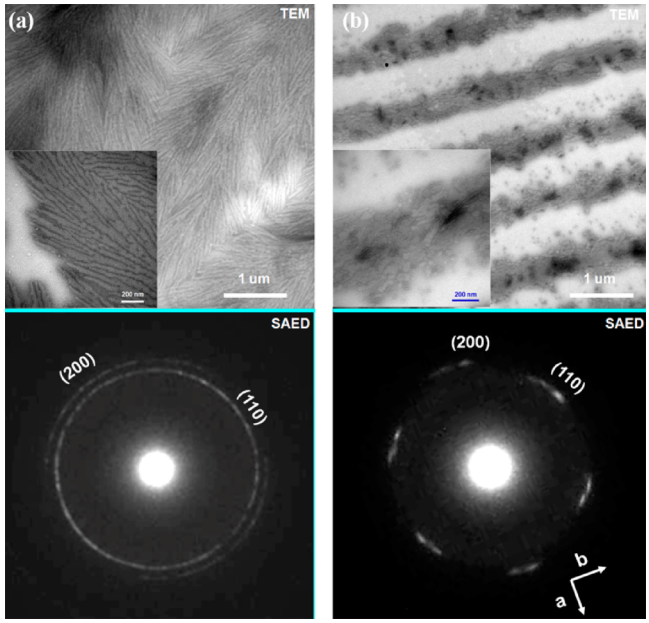

Figure 3. TEM images and corresponding SAED patterns of the (a) unmolded and (b) molded PB-*b*-PCL thin films. The insets in panels a and b (stained with osmium tetraoxide) show the high-resolution structures and the Cartesian coordinate system, in the lower-right corner of panel b, shows the orientation of crystallographic a and *b*-axis.

crystallization morphology changed from dendrites (panel a) to regular lines (panel b) after micromolding. In addition, dark area corresponds to high electron-density and enrichment of the material. As shown in Figure 3b (inset of panel b shows the high-resolution image), the molded lines (dark zones) are separated by clear white gaps, suggesting that the material was well confined in the molded lines. We primarily anticipated that less cross-channel crystallization took place in the micromolded PB-*b*-PCL thin film. Furthermore, select area electron diffraction (SAED) was applied to characterize the crystal orientation and the results are shown below the corresponding TEM images. For analysis of the SAED result, we should note that the diffraction pattern of the orthorhombic PCL crystal mainly consisted of six spots, two (200) planes and four (110) planes.[29] In Figure 3a, (110) and (200) diffraction circles are discerned, indicating the crystalline lamellae were in flat-on orientation. Furthermore, the SAED result also tells that the lamellae did not show regular arrangement.

As shown in Figure 3b, symmetric (110) and (200) diffraction spots are observed in the micromolded PB-*b*-PCL thin film, indicating the lamellae take a flat-on orientation. An in-depth analysis was undertaken by comparing the crystallo-

dx.doi.org/10.1021/mz3002758 | *ACS Macro Lett.* 2012, 1, 1007−1011

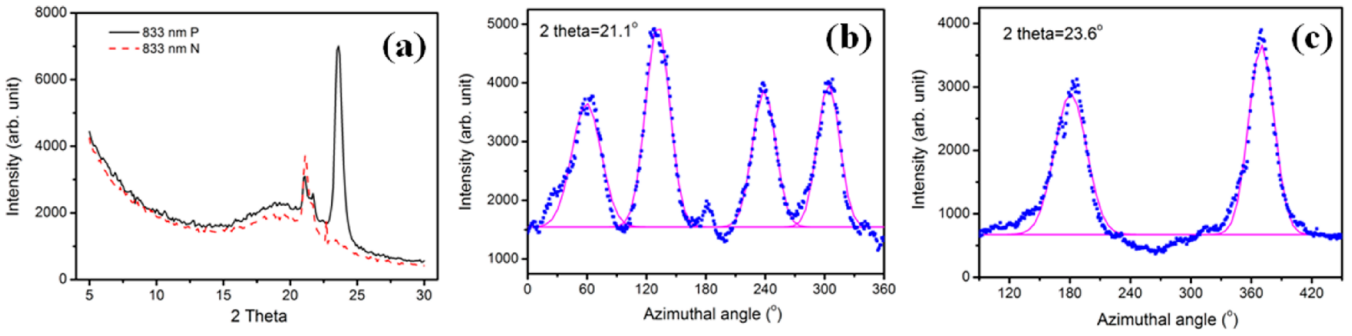

Figure 4. (a) Intensity profiles of the 2θ scanning for the in-plane GIXRD of the molded PB-*b*-PCL thin film. P and N correspond to the scanning directions parallel and normal to the long-axis of the channels, respectively. Intensity profiles of the Φ scanning with the 2θ locked at (b) 21.1 and (c) 23.6° for the in-plane GIXRD of the micromolded PB-*b*-PCL thin film. The Φ scanning started from the direction normal to the long-axis of the channel. The experimental results were fitted with Gaussian equation as indicated by the solid lines.

graphic *a*-axis, indicated by (200) diffraction plane, with the long-axis of the channels. Clearly, they were nearly perpendicular to each other. As reported in the previous publications, the PCL crystallized into an orthorhombic crystal lattice irrespective of the confinements.[6,24,26,27,30] Therefore, it was easy to infer that the crystallographic *b*-axis (fast growth direction[23,26]) was nearly parallel to the long-axis of the channels. This alignment was favored for geometric reasons, and analogous crystal orientation was detected in ref 5, where polyethylene crystal extended along the long-axis of the channel, because it allowed the crystals to grow long in a direction.

As mentioned above, AFM and TEM detected that the material was well confined in the molded lines, and SAED experimental results verified that crystallographic *b*-axis of PCL crystal was nearly parallel to the long-axis of the channel. We were, naturally, curious to find out whether the preferential crystallization structure would present a long-range ordering feature. To find out, grazing-incidence X-ray diffraction (GIXRD; obtained at 1W1A, Beijing Synchrotron Radiation Facility using a Huber 5-circle diffractometer and a point detector) was applied. The horizontal and vertical slit sizes of the spot on the sample were about 0.4 (width) and 251 (length) mm, which was big enough to represent statistically the long-range ordering of the PCL crystals. The ideal X-ray penetration depth with incident angle (α_i) 0.16° was calculated (Supporting Information), and the result revealed that the X-ray penetration depth was much larger than the film thickness. Thus, the GIXRD reflected the crystallization information from the polymer−air interface to the polymer−substrate interface. Furthermore, to set the position (see Figure S2 of the Supporting Information), the long-axis of the channel was first marked with the optical microscope (Carl Zeiss A2m microscope), then, it was set normal (N) or parallel (P) to the incident X-ray.

Figure 4 shows the in-plane GIXRD results. As shown in Figure 4a, the profiles have two dominant sharp peaks at 2θ = 21.1 and 23.6°, respectively. In contrast, there was no distinguishable diffraction peak detected in the out-of-plane GIXRD experimental result (not shown here). Therefore, GIXRD experimental results proved that only flat-on crystal lamellae existed in the sample. The present findings agreed well with the TEM and SAED experimental results, that is, flat-on lamellae formed. In addition, 2θ = 23.6° peak was found only in the P direction, indicating that the crystal orientation showed anisotropy.

To give a quantitative characterization of the crystal anisotropic orientation, the azimuthal intensity profiles of the 2θ = 21.1 and 23.6° reflections were detected, and related results are shown in Figure 4b and c, respectively. Figure 4b reveals that the 2θ = 21.1° reflection has four maxima, that is, Φ = 61°, 128°, 238°, and 305°. Figure 4c exhibits that 2θ = 23.6° reflection has two maxima, that is, Φ = 182° and 371°. It should be noted that the peak fitting (indicated by the solid lines) was undertaken with Origin 6.0 (Origin Lab Cor.), assuming the Gaussian function for each diffraction peak. On the basis of the Bragg equation and the fact that PCL belongs to orthorhombic system (lattice constants *a* = 0.745 nm, *b* = 0.498 nm, and *c* = 1.705 nm),[27] the 2θ = 21.1 and 23.6° peaks were attributed to (110) and (200) reflections, respectively. Furthermore, for cylindrically confined PCL with the crystallographic *b*-axis parallel to the long-axis of the cylinders, it was reported that the azimuthal angles of the (110) diffraction would appear at 58°, 122°, 238°, and 302°, and those of the (200) diffraction would appear at 0° and 180°.[6] These reported azimuthal-angle values agreed well with our experimental results presented here, suggesting that PCL crystals in the micromolded PB-*b*-PCL thin film exhibited analogous preferential orientation to that confined in a cylindrical microphase structure. Therefore, the GIXRD experimental results undoubtedly revealed that the PCL crystal arrangement showed long-range ordering feature.

So far, we detected that the crystalline lamellae in the micromolded PB-*b*-PCL thin film had long-range ordering feature. To the best of our knowledge, this is the first time for soft-confined block copolymer in thin films that the long-range ordered crystallization structure was prepared; it was interesting to explore the inherent mechanism. First of all, we noted that the crystallization of PCL homopolymer was less influenced by the geometric effect. As shown in the in-plane GIXRD experimental results of the micromolded PCL thin film (see Figure S3 of the Supporting Information), there are two dominant peaks ((110) and (200) diffraction peaks) in both P and N directions, indicating that there was no preferential crystallographic orientation. Comparing PB-*b*-PCL diblock copolymer with PCL homopolymer, there was not only less crystallizing species, but also retarded molecular diffusion because of the microphase structure confinement. Second, it was reported that the preferential crystallographic orientation of PCL in hard-confined microdomains was generally prepared in more rigorous conditions, for example, Nojima et al. reported that, in the PS/PCL system, the crystallographic *b*-axis was paralleling to the long-axis of the channel only when the

dx.doi.org/10.1021/mz3002758 | *ACS Macro Lett.* 2012, 1, 1007−1011

diameter of the crystallizing cylinders was no more than 13 nm.[6,24] Similar diameter effect has also been reported for homopolymer crystallization in the porous templates.[21,22] We also realized that geometric confinement effect could promote the orientation of cylindrical microdomains of block copolymers that are parallel to the channel, even though the width of the channels lies in a few hundred nanometers.[13,31] In our case, the phase-separated cylindrical domains with adiameter of about 6.1 nm (calculated from the amorphous bulk periodicity, 18.7 nm,[28] by the f_{PCL}) may be oriented in the confined geometry before the crystallization takes place. It would be confirmed in the future experiments. If this is true, it is natural to understand that the PCL crystal would extend along the long-axis of the channels because crystallizing species enriched in this direction.

Furthermore, as mentioned in the partially confined homopolymer thin films, the residual layer could deliver crystallization between different channels, and spherulite was generally detected.[14,15,18] As shown in panel b of Figure 1, we also detected a residual layer, with the thickness comparable to the half-periodicity value of the crystallized PB-*b*-PCL (ca. 32.4 nm[28]) around the substrate. However, the block copolymer is quite different from the homopolymer, because the "in-plane" molecular diffusion in the thin residual layer was restricted by the ordering of the diblock copolymer induced by the SiOx/Si substrate, where the substrate would affine the PCL block due to favorable interaction.[32] Therefore, cross-channel crystallization was precluded and spherulite was absent in the micromolded PB-*b*-PCL thin film.

In summary, under the help of micromolding, we successfully prepared a preferentially oriented crystal structure in a semicrystalline diblock copolymer thin film. The long-range ordered structure with a crystallographic *b*-axis nearly parallel to the long-axis of the channel was indicated by the AFM, TEM, SAED, and GIXRD experimental results. It was illustrated that micromolding introduced designed physical constraints into the PB-*b*-PCL thin film, which determined the melt flow and directed the crystallization. Compared with the micromolded PCL thin film, the success of preparing a long-range ordered crystallization structure in the micromolded PB-*b*-PCL thin film was closely related to the preferentially aligned microdomains, because the crystallizing species enriched in the direction parallel to the long-axis of the channel which yielded the fast-growth axis extended along this direction. Furthermore, the substrate-induced ordering of the block copolymer restricted the cross-channel crystallization and no spherulite was detected in the micromolded PB-*b*-PCL thin film. The experimental results presented here imply that the long-range ordered crystallization structures in block copolymers thin film could be prepared through micromolding, which is simple and cost-efficient.

■ ASSOCIATED CONTENT

Ⓢ Supporting Information

Calculation of the X-ray penetration depth in PB-*b*-PCL (S1); Optical microscope image of the molded PB-*b*-PCL thin film (Figure S2); In-plane GIXRD experimental results of the micromolded PCL thin film (Figure S3). This material is available free of charge via the Internet at http://pubs.acs.org.

■ AUTHOR INFORMATION

Corresponding Author

*E-mail: tbhe@ciac.jl.cn; zhijun.hu@suda.edu.cn.

Notes

The authors declare no competing financial interest.

■ ACKNOWLEDGMENTS

A portion of this work is based on the data obtained at 1W1A, BSRF. The authors gratefully acknowledge the assistance of scientists of Diffuse X-ray Scattering Station during the experiments. This work is supported by the National Science Foundation of China (No. 21074135). Z.H. thanks the financial support of National Science Foundation of China (Nos. 21074084 and 91027040), the Natural Science Foundation of Jiangsu Province of China (No. BK2010213), the Opening Project of the State Key Laboratory of Polymer Physics and Chemistry (China), and a Project Funded by the Priority Academic Program Development of Jiangsu Higher Education Institutions (PAPD).

■ REFERENCES

(1) Wunderlich, B. *Macromolecular Physics*; Academic Press: New York, 1976.
(2) Hsiao, M. S.; Chen, W. Y.; Zheng, J. X.; Van Horn, R. M.; Quirk, R. P.; Ivanov, D. A.; Thomas, E. L.; Lotz, B.; Cheng, S. Z. D. *Macromolecules* **2008**, *41*, 4794.
(3) Loo, Y. L.; Register, R. A.; Ryan, A. J.; Dee, G. T. *Macromolecules* **2001**, *34*, 8968.
(4) Loo, Y. L.; Register, R. A.; Ryan, A. J. *Phys. Rev. Lett.* **2000**, *84*, 4120.
(5) Quiram, D. J.; Register, R. A.; Marchand, G. R.; Adamson, D. H. *Macromolecules* **1998**, *31*, 4891.
(6) Nojima, S.; Ohguma, Y.; Kadena, K.; Ishizone, T.; Iwasaki, Y.; Yamaguchi, K. *Macromolecules* **2010**, *43*, 3916.
(7) Sun, Y. S.; Chung, T. M.; Li, Y. J.; Ho, R. M.; Ko, B. T.; Jeng, U. S.; Lotz, B. *Macromolecules* **2006**, *39*, 5782.
(8) Muller, A. J.; Balsamo, V.; Arnal, M. L.; Jakob, T.; Schmalz, H.; Abetz, V. *Macromolecules* **2002**, *35*, 3048.
(9) Heier, J.; Kramer, E. J.; Groenewold, J.; Fredrickson, G. H. *Macromolecules* **2000**, *33*, 6060.
(10) Huang, P.; Guo, Y.; Quirk, R. P.; Ruan, J.; Lotz, B.; Thomas, E. L.; Hsiao, B. S.; Avila-Orta, C. A.; Sics, I.; Cheng, S. Z. D. *Polymer* **2006**, *47*, 5457.
(11) Massa, M.; Carvalho, J.; Dalnoki-Veress, K. *Phys. Rev. Lett.* **2006**, *97*, 247802.
(12) Carvalho, J.; Dalnoki-Veress, K. *Eur. Phys. J. E* **2011**, *34*, 1.
(13) Fitzgerald, T. G.; Farrell, R. A.; Petkov, N.; Bolger, C. T.; Shaw, M. T.; Charpin, J. P. F.; Gleeson, J. P.; Holmes, J. D.; Morris, M. A. *Langmuir* **2009**, *25*, 13551.
(14) Hu, Z.; Baralia, G.; Bayot, V.; Gohy, J.; Jonas, A. *Nano Lett.* **2005**, *5*, 1738.
(15) Hu, Z. J.; Jonas, A. M. *Soft Matter* **2010**, *6*, 21.
(16) Hu, Z.; Tian, M.; Nysten, B.; Jonas, A. *Nat. Mater.* **2009**, *8*, 62.
(17) Hu, Z.; Muls, B.; Gence, L.; Serban, D.; Hofkens, J.; Melinte, S.; Nysten, B.; Demoustier-Champagne, S.; Jonas, A. *Nano Lett.* **2007**, *7*, 3639.
(18) Okerberg, B. C.; Soles, C. L.; Douglas, J. F.; Ro, H. W.; Karim, A.; Hines, D. R. *Macromolecules* **2007**, *40*, 2968.
(19) Shin, K.; Woo, E.; Jeong, Y. G.; Kim, C.; Huh, J.; Kim, K. W. *Macromolecules* **2007**, *40*, 6617.
(20) Woo, E.; Huh, J.; Jeong, Y. G.; Shin, K. *Phys. Rev. Lett.* **2007**, *98*, 136103.
(21) Steinhart, M.; Goring, P.; Dernaika, H.; Prabhukaran, M.; Gosele, U.; Hempel, E.; Thurn-Albrecht, T. *Phys. Rev. Lett.* **2006**, *97*, 027801.
(22) Wu, H.; Wang, W.; Huang, Y.; Su, Z. *Macromol. Rapid Commun.* **2009**, *30*, 194.
(23) Mareau, V.; Prud'Homme, R. *Macromolecules* **2005**, *38*, 398.
(24) Nakagawa, S.; Kadena, K.-i.; Ishizone, T.; Nojima, S.; Shimizu, T.; Yamaguchi, K.; Nakahama, S. *Macromolecules* **2012**, *45*, 1892.

(25) Nojima, S.; Kato, K.; Yamamoto, S.; Ashida, T. *Macromolecules* **1992**, *25*, 2237.
(26) Beekmans, L.; Vancso, G. *Polymer* **2000**, *41*, 8975.
(27) Chatani, Y.; Okita, Y.; Tadokoro, H.; Yamashit., Y *Polym. J.* **1970**, *1*, 555.
(28) Zhang, P.; Huang, H.; Yan, D.; He, T. *Langmuir* **2012**, *28*, 6419.
(29) Wang, Z. B.; Alfonso, G. C.; Hu, Z. J.; Zhang, J. D.; He, T. B. *Macromolecules* **2008**, *41*, 7584.
(30) Qiao, C.; Zhao, J.; Jiang, S.; Ji, X.; An, L.; Jiang, B. *J. Polym. Sci., Part B: Polym. Phys.* **2005**, *43*, 1303.
(31) Park, S. M.; Liang, X. G.; Harteneck, B. D.; Pick, T. E.; Hiroshiba, N.; Wu, Y.; Helms, B. A.; Olynick, D. L. *ACS Nano* **2011**, *5*, 8523.
(32) Green, P. F.; Limary, R. *Adv. Colloid Interface Sci.* **2001**, *94*, 53.